Supplemental Materials

Isolation of ECs from hearts

Primary cultures of mouse cardiac microvascular ECs (MCMEC) were prepared by combined methods of previous articles[1, 2]. Six hearts were isolated from six adult mice of wild type C57Bl/6j. After the aorta, valves, atria and right ventricle were removed, epicardial and endocardial endothelial cells were devitalized by immersing the left ventricles in 70% EtOH for 10 sec, followed by extensive washing with PBS. The left ventricles were minced finely in 35 ml of DMEM containing collagenase (0.4 mg/ml) and dispase (1.5 mg/ml), followed by incubation for 60 min at 37^{o}C in a stirrer. After the filtration of the dissociated cells through a nylon mesh filter, cells were collected by centrifugation at 1,000 rpm for 10 min and the pellet was resuspended in 1 ml of DMEM. The suspension was overlaid onto the density gradient of 30% Percoll and was centrifuged at 15,000 rpm for 10 min. The microvessel endothelial cells and fibroblasts (the middle layer from three layers) were suspended in culture medium (EBM-2; Lonza Walkersville Inc, Maryland), plated onto collagen type-I coated dish and maintained at 37^{o}C in a 5% CO_2 incubator until use. Cells were fixed with 4% paraformaldehyde, permeabilized with 0.1% Triton X, and co-incubated with two antibodies against FABP4 and PECAM (R&D), followed by co-staining with two secondary antibodies, anti-rabbit IgG conjugated with Cy3 (Sigma Aldrich) and anti-goat IgG conjugated with Alexa fluor 488 (Invitrogen). Nuclei were stained with 4',6-diamino-2-phenylindole (Wako Chemical, Osaka). Signals were observed by BIOREVO microscopy (Keyence).

Echocardiography

In vivo cardiac function was assessed by transthoracic echocardiography (EUB-7500, Hitachi) in conscious mice. M-mode LV end-systolic and end-diastolic dimensions were averaged from 3–5 beats. LV percent ejection fraction and fractional shortening were calculated as described previously [3].

Supplemental figure legends

Figure SI

(A) Expression of mRNA for *Fabp4* and *Fabp5* in various organs of WT mice. The number of cycles is indicated on the right. GAPDH is used as internal control. (B and C) Immunohistochemical localization of FABP4 and FABP5 in indicated organs from wild type, *Fabp4* (-/-), *Fabp5* (-/-) and *Fabp4/5* DKO mice. Ao; aorta, BAT; brown adipose tissue. Note that FABP5 is also expressed in endocardial cells. (D) Double immunofluorescence of FABP4 (red) with isolectin B4, an endothelial marker (green), in indicated organs of WT mice. Nuclei were stained with DAPI (blue). (E) Double immunofluorescence of FABP4 (red) with PECAM, an endothelial marker (green), in primary culture that was prepared from hearts from WT mice. (F) Double immunofluorescence of FABP5 (red) with isolectin B4 (green) in white adipose tissue of WT and *Fabp4* (-/-) mice. Nuclei were stained with DAPI (blue). (G) Immunohistochemical localization of FABP4 and FABP5 in human heart and adipose tissue. (H) Immunohistochemical localization of PECAM/CD31 (R&D), FABP4 and FABP5 in the heart at different developmental stages. (I) No expression of FABP4 and FABP5 in capillary ECs in liver, brain and lungs of wild type mice. Note that FABP5 is expressed in type II alveolar cells and macrophages in the lung [4].

Figure SII

(A to D) Uptake of ^{125}I-BMIPP (A and C) and ^{18}F-FDG (B and D) by indicated tissues from WT, *Fabp4(-/-), Fabp5(-/-)* and *Fabp4/5* DKO mice after a 24-hour fast with or without 2-hour refeeding (n=6). (A and B) male, (C and D) female. *P<0.05, **P<0.01, ***P<0.001. Bld; blood, Liv; liver, Hrt; heart, R-M; red skeletal muscle, W-M; white skeletal muscle, Fat; gonadal fat pad, S; soleus, D; diaphragma, Q; quadriceps, G; gastrocnemius. (E) Uptake of ^{18}F-FDG by indicated tissues from WT or *Fabp4/5* DKO mice (n=6). A part of figures 2B and S2D is shown in small scale. *P<0.05, **P<0.01. (F) The uptake of ^{125}I-BMIPP and ^{18}F-FDG by tissues from WT or *Fabp4/5* DKO mice during the fed state (n=4). *P<0.05, **P<0.01, ***P<0.001. (G) Representative MIP PET image of ^{18}F-FDG 2 hours after injection in WT and *Fabp4/5* DKO mice after a 24-hour fast. MIP: maximum intensity projection. Note that the MIP image excludes the possibility that the intensity of ^{18}F-FDG that is observed by conventional methods (figure 2C) is caused by slice level.

Figure SIII

Expression of genes associated with glucose metabolism in hearts.

Relative mRNA expression of genes that were associated with glucose metabolism in the hearts of WT and *Fabp4/5* DKO mice was examined by semi-quantitative PCR with or without a

24-hour fast. Slc2a4; solute carrier family 2 member 4 (Glut4), Pfkm; phosphofructokinase muscle (Pfk1), Pfkfb3; 6-phosphofructo-2-kinase/fructose-2,6-biphosphatase 3 (Pfk2), Pdha1; pyruvate dehydrogenase alpha 1, Pdhb; pyruvate dehydrogenase beta, Pdhx; pyruvate dehydrogenase complex, component X.

Figure SIV

Metabolome analysis of *Fabp4/5* DKO hearts. AMP from the hearts of WT and *Fabp4/5* DKO mice after a 24-hour fast were measured by capillary electrophoresis-mass spectrometry (n=6). The ratio of AMP/ATP was calculated.

Figure SV

The expression of markers for cardiac overload was detected by real-time PCR. ANP; atrial natriuretic peptide, BNP; brain natriuretic peptide, α-MHC; myosin heavy chain 6 (cardiac muscle, alpha), β-MHC; myosin heavy chain 7 (cardiac muscle, beta).

Figure SVI

Plausible mechanism of FA and glucose metabolism in the heart of *Fabp4/5* DKO mice. In *Fabp4/5* DKO hearts, FA uptake is reduced due to impaired trans-endothelial FA transport, whereas glucose uptake is dramatically promoted even during fasting to compensate for a shortage of ATP production independently of insulin. Glucose uptake is increased by the upregulated expression of Glut4 at the post-transcriptional level. The glycolysis pathway is accelerated by the allosteric regulation of PFK1 due to a decrease in the rate of ATP production and an increase in Fru-2,6-P2. Partial acetyl CoA, which is derived from glucose, serves as materials of FA synthesis, leading to insufficient supply of acetyl CoA for ATP production. This scenario can account for the striking magnitude of glucose uptake relative to the reduction of FA uptake in DKO hearts during fasting. The concentration of ketone bodies (β-hydroxybutyrate) in serum and heart is higher in DKO mice than WT, suggesting that the ketone body utilization pathway largely contributes to the source of ATP production in DKO hearts during fasting. See the Results and Discussion sections in detail.

Supplemental References

1. Nishida M, Carley WW, Gerritsen ME, Ellingsen O, Kelly RA, Smith TW. Isolation and characterization of human and rat cardiac microvascular endothelial cells. *Am J Physiol*. 1993;264:H639-652
2. Saito T, Shibasaki K, Kurachi M, Puentes S, Mikuni M, Ishizaki Y. Cerebral capillary endothelial cells are covered by the vegf-expressing foot processes of astrocytes. *Neurosci Lett*. 2011;497:116-121
3. Koitabashi N, Danner T, Zaiman AL, Pinto YM, Rowell J, Mankowski J, Zhang D, Nakamura T, Takimoto E, Kass DA. Pivotal role of cardiomyocyte tgf-beta signaling in the murine pathological response to sustained pressure overload. *J Clin Invest*. 2011;121:2301-2312
4. Owada Y, Abdelwahab SA, Suzuki R, Iwasa H, Sakagami H, Spener F, Kondo H. Localization of epidermal-type fatty acid binding protein in alveolar macrophages and some alveolar type ii epithelial cells in mouse lung. *Histochem J*. 2001;33:453-457

Supplemental figure I

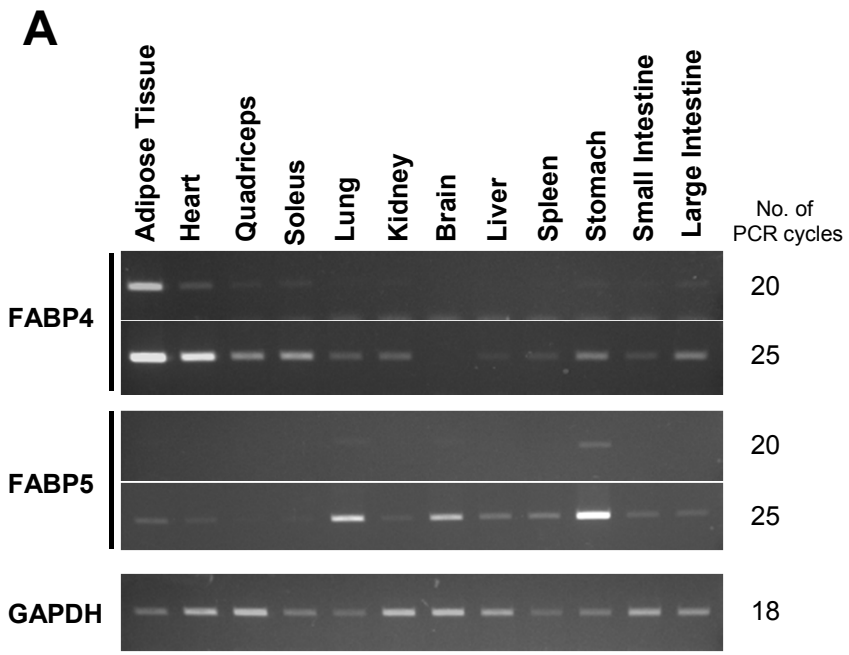

Supplemental figure I

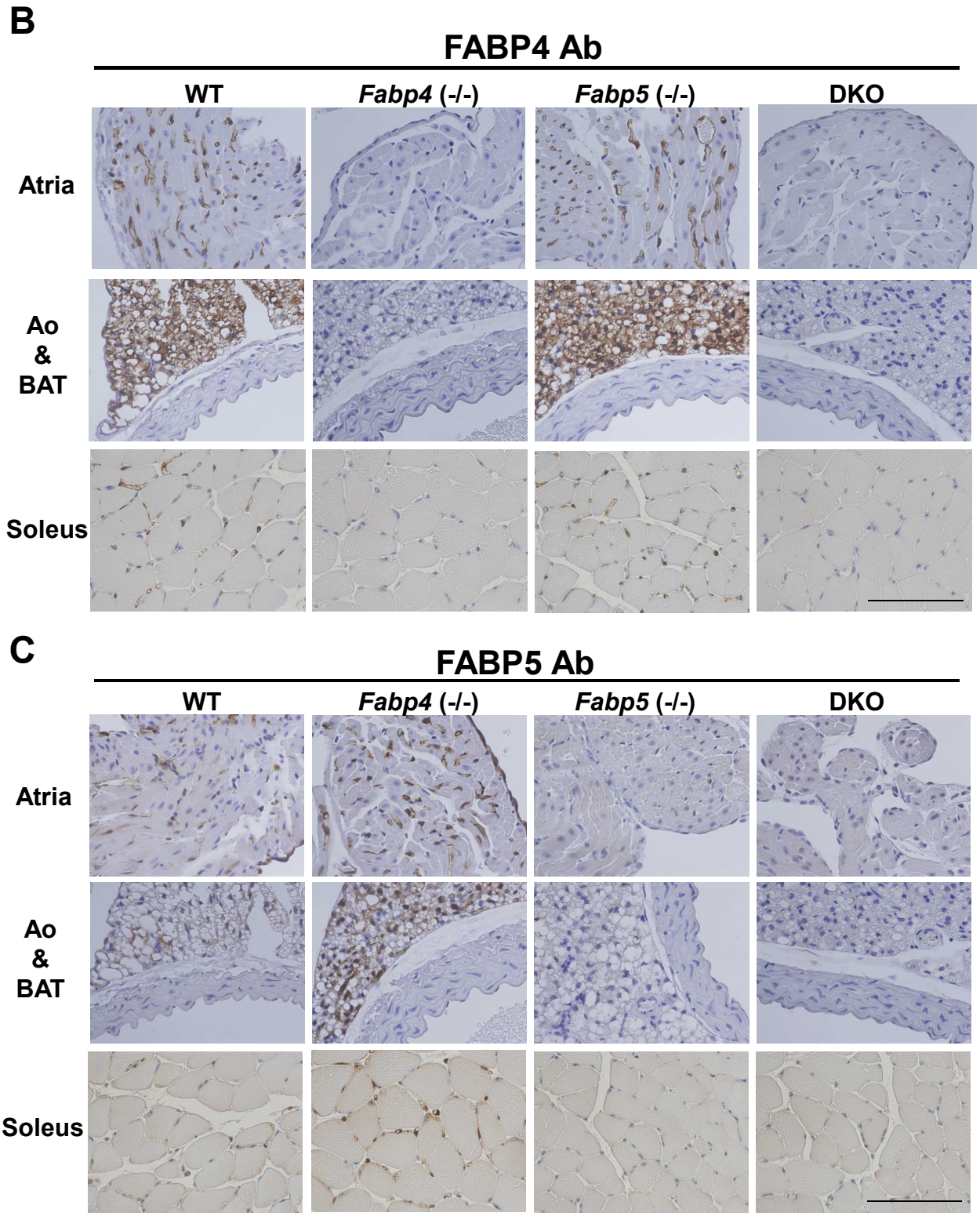

Supplemental figure I

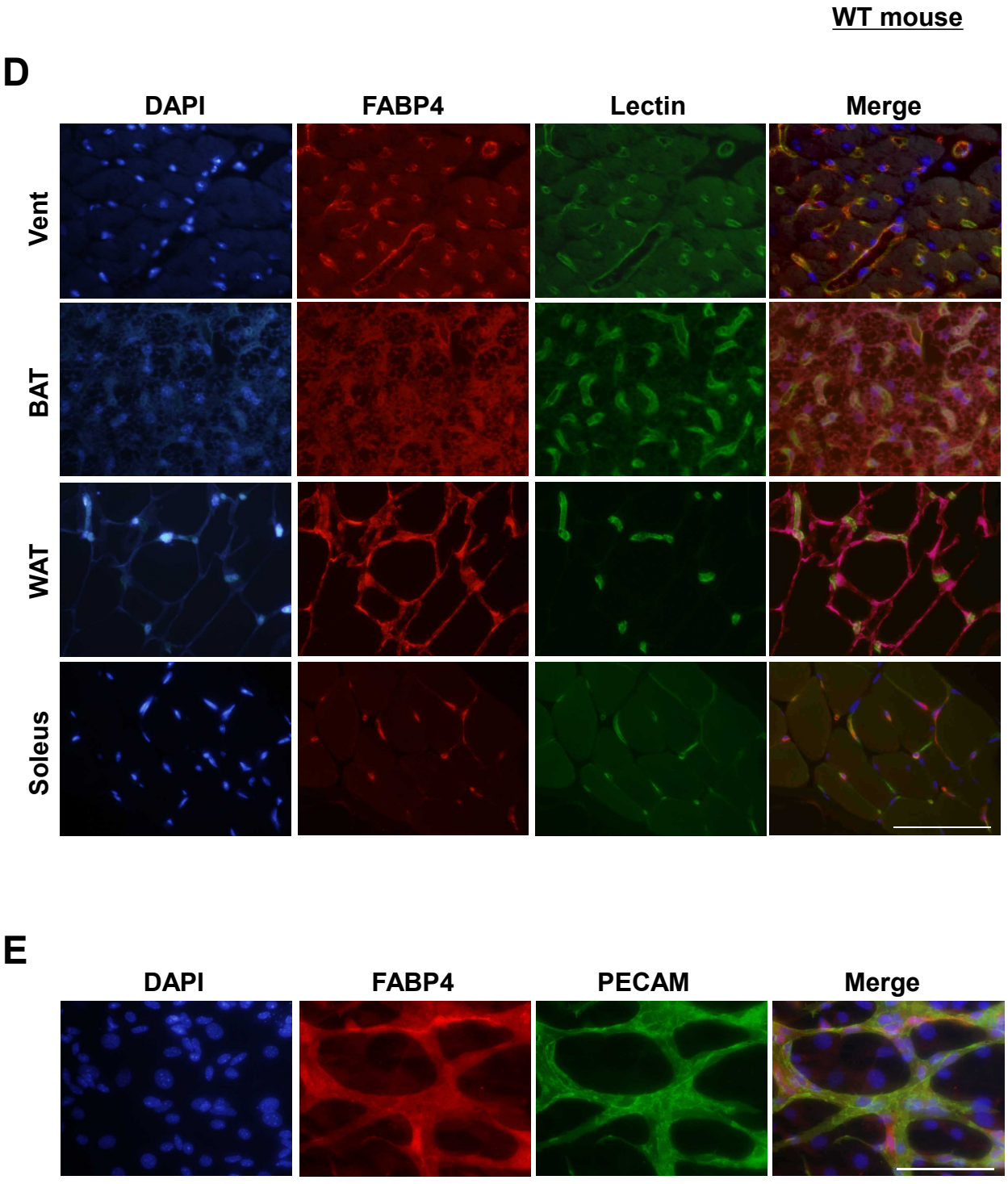

Supplemental figure I

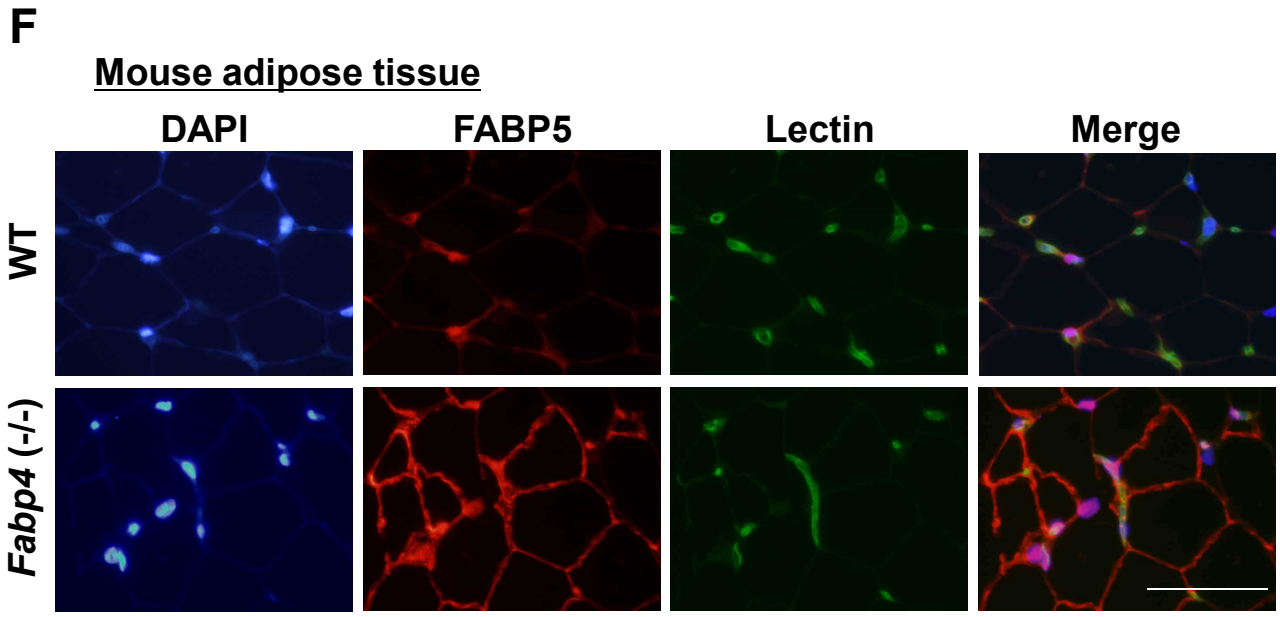

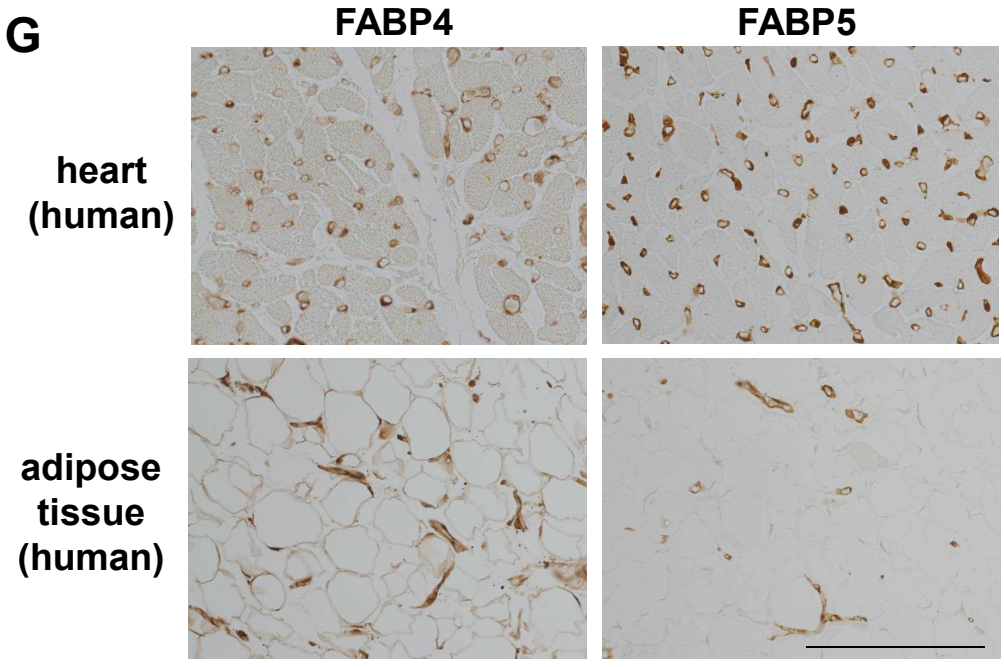

Supplemental figure I

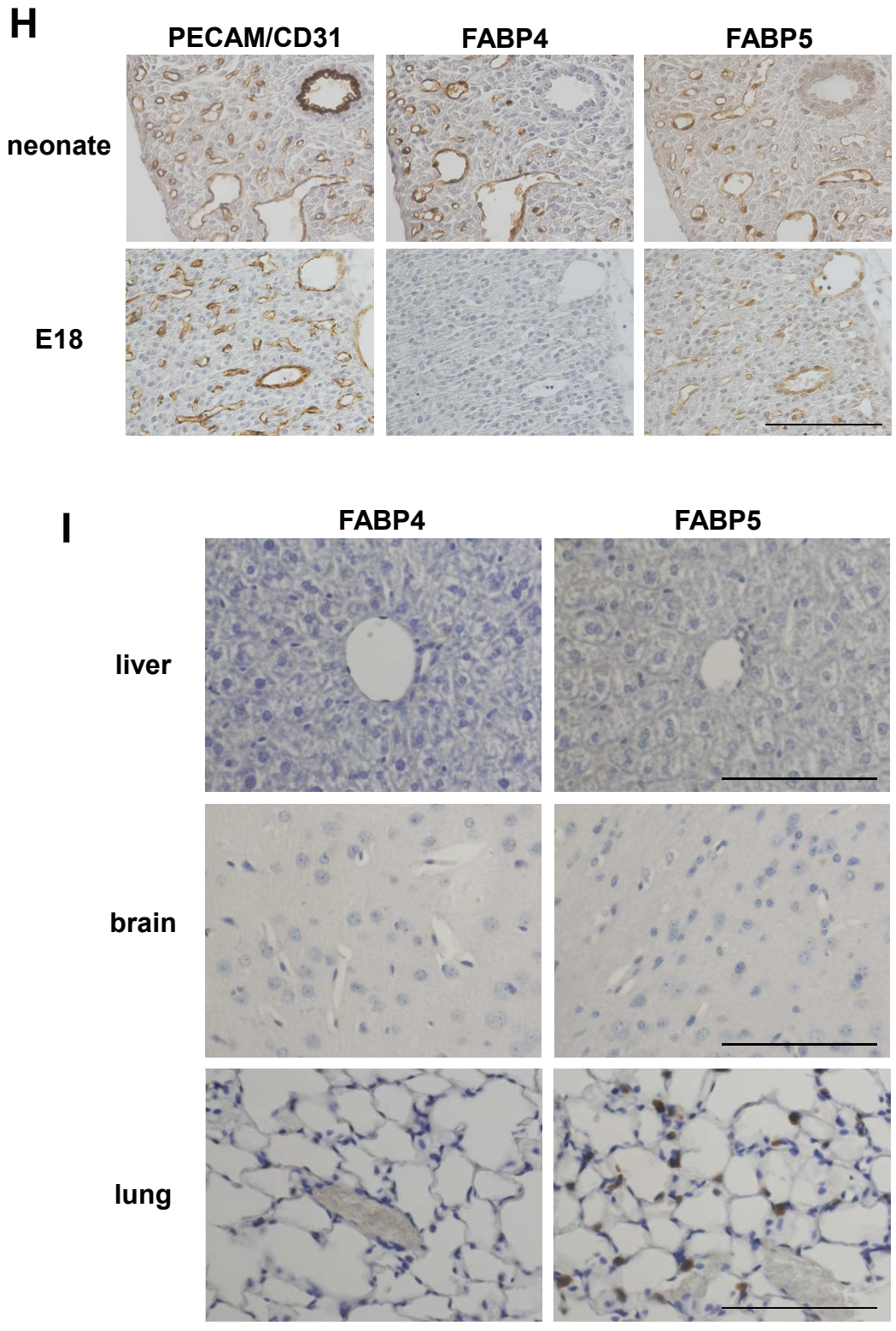

Supplemental figure II

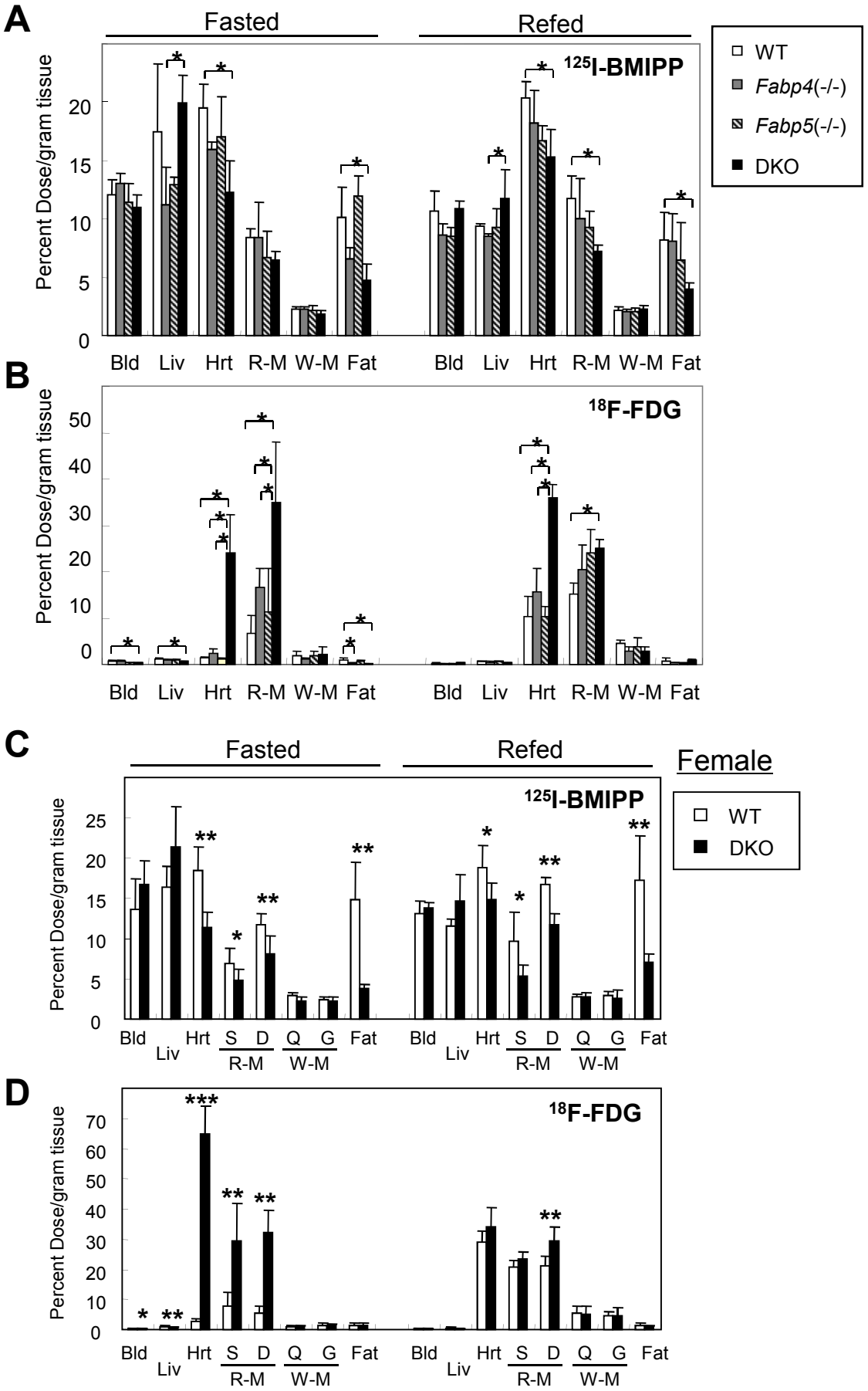

Supplemental figure II

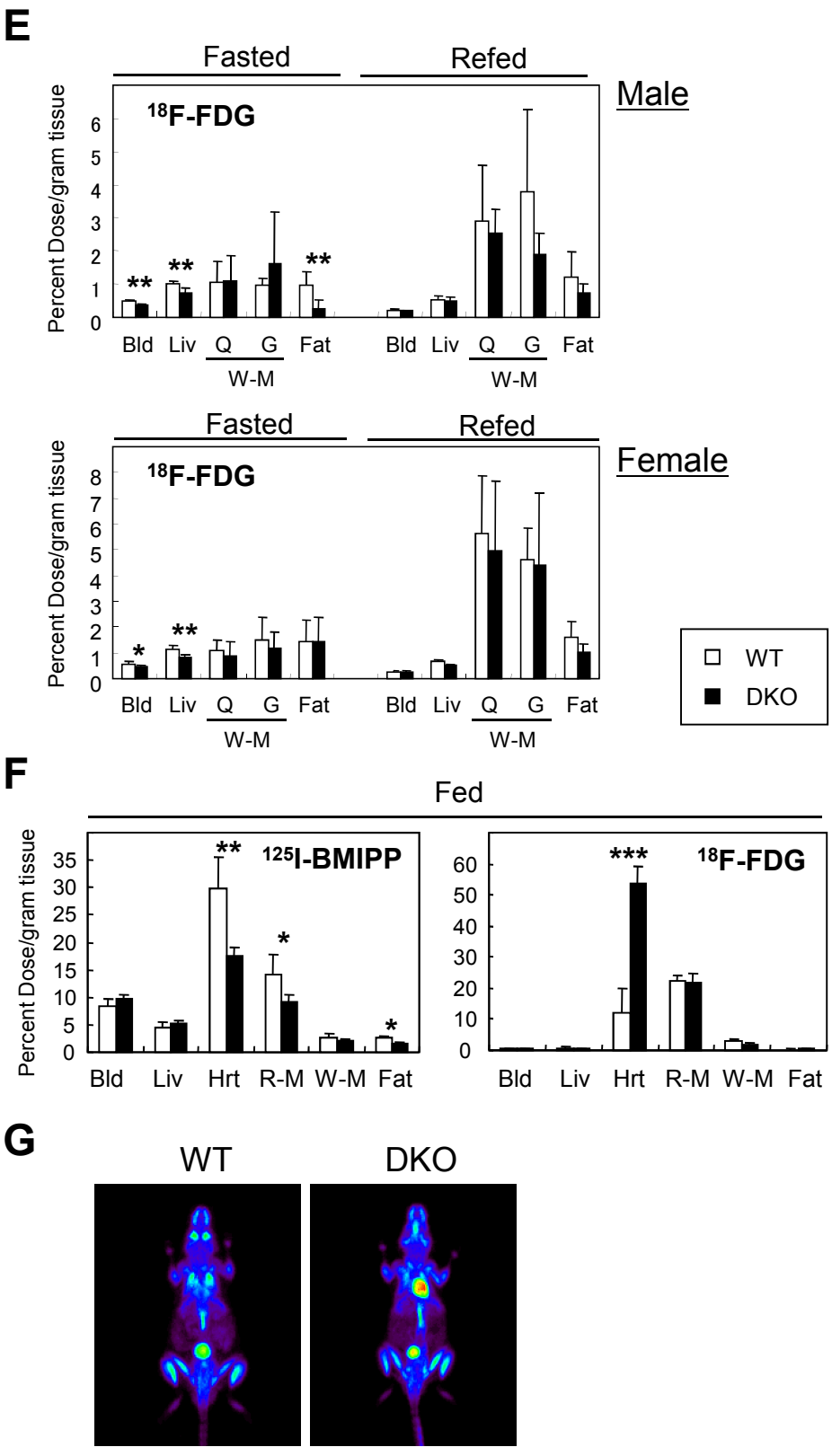

Supplemental figure III

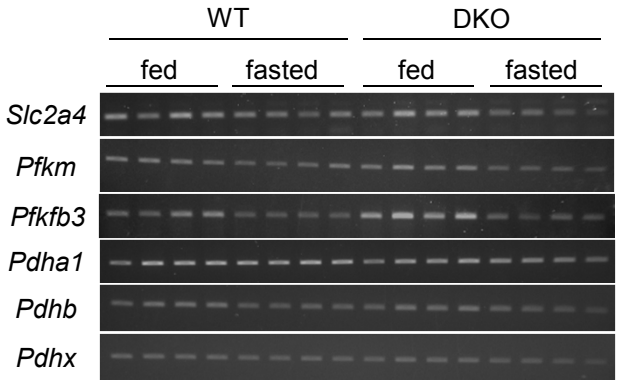

Supplemental figure IV

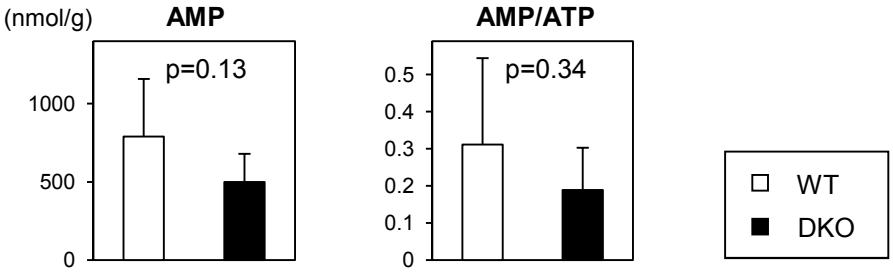

Supplemental figure V

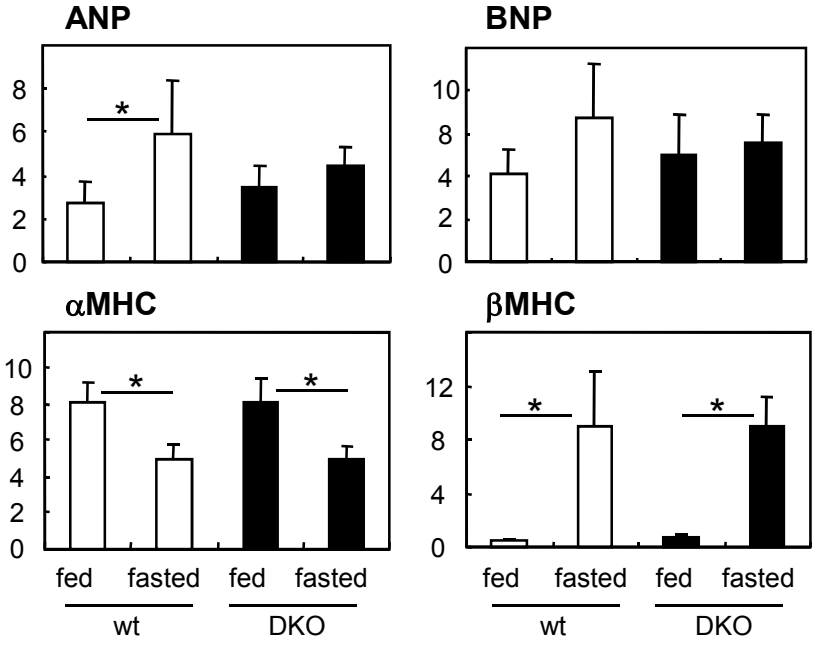

Supplemental figure VI

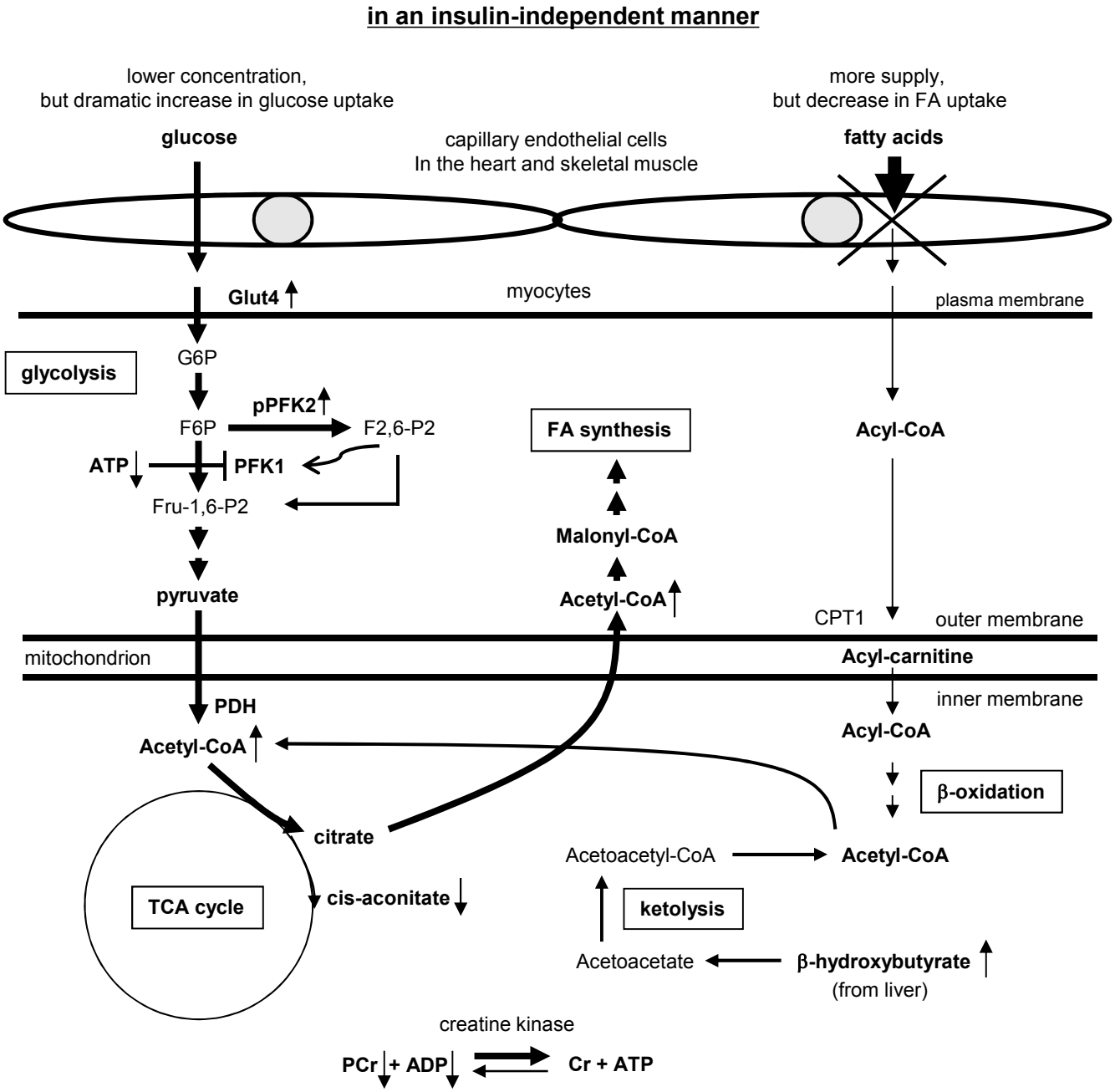

Supplemental Table I. Primers for RT-PCR

	forward	reverse
ANP	cctgtgtacagtgcggtgtc	aagctgttgcagcctagtcc
BNP	gccagtctccagagcaattc	ccgatccggtctatcttgtg
aMHC	agctggagaatgagctggag	ggttattcctcgtcgtgcat
bMHC	gaagggcatgaggaagagtg	ggagctgggtagcacaagag
Acadm (Mcad)	ggcaaatgcctgtgattctt	acccattgcgatcttgaaac
Acadl (Lcad)	acttgggaagagcaagcgta	ttccgttttccaccaaaaag
Cd36 (Fat)	tgctggagctgttattggtg	tgggttttgcacatcaaaga
Cpt1b	gtcgcttcttcaaggtctgg	aagaaagcagcacgttcgat
Cpt2	tcctcgatcaagatgggaac	gatccttcatcgggaagtca
Fabp3	catcgagaagaacggggata	tgccatgagtgagagtcagg
Fabp4	aagaagtgggagtgggcttt	tcgactttccatcccacttc
Fabp5	caaaaccgagagcacagtga	tttgaccgctcactgaattg
Gapdh	accacagtccatgccatcac	tccaccaccctgttgctgta
Lpl	gcccagcaacattatccagt	ggtcagacttcctgctacgc
Pdha1	atgcacatgtacgccaagaa	tgtgtccatggtagcggtaa
Pdhb	gtgtagctgctcagcactcg	actggtcttgaatgggcaac
Pdhx	agctgccctctgttgacatt	cttcatcctccgtcagcttc
Pdk4	aaagatgctctgcgaccagt	cctgcttgggatacaccagt
Pfkm (Pfk1)	cgagacgatgggtggttact	ccccagaacacaacctgagt
Pfkb3 (Pfk2)	ctataaaccccacgcctcaa	gcaatctgcccactctcttc
Slc2a4 (Glut4)	gattctgctgcccttctgtc	attggacgctctctctccaa
Ucp2	aaggggagagtcaagggcta	tgtcatgaggttggctttca
Ucp3	gtccgatttcaagccatgat	aaaggagggcacaaatcctt

Supplemental Table II. Body weight, heart weight and vital signs

	male		female	
	WT	DKO	WT	DKO
body weight (g)	25.7 ± 2.3	24.9 ± 1.9	20.2 ± 1.4	19.7 ± 1.3
heart weight (mg)	109.2 ± 3.2	116.7 ± 7.7*	82.0 ± 4.1	89.2 ± 7.1*
HW/BW (mg/g)	4.28 ± 0.14	4.68 ± 0.06*	4.07 ± 0.15	4.53 ± 0.21*
systolic BP (mmHg)	95.3 ± 6.0	100.2 ± 8.6	88.4 ± 9.2	94.4 ± 10.3
heart rate (bpm)	675 ± 14	684 ± 14	673 ± 25	672 ± 36

Mice are 12-week-old. Number of mice in each group is eight.
HW/BW; heart weight/body weight ratio, BP: blood pressure, bpm; beat per minute.
The values shown are means ± SD. *$p < 0.05$ versus WT

Supplemental Table III. Echocardiographic data

	WT	DKO
LVDd (mm)	3.09 ± 0.17	2.96 ± 0.16
LVDs (mm)	1.75 ± 0.12	1.71 ± 0.06
ejection fraction (%)	81.2 ± 2.9	80.1 ± 1.9
fractional shortening (%)	43.9 ± 3.02	42.6 ± 1.83

Cardiac function of 12-week-old mice was estimated by trans-thoracic echocardiography. Number of mice in each group is eight. LVDd; left ventricle diastolic diameter, LVDs; left ventricle systolic diameter. The values shown are means ± SD. There was no significant difference between each group.